WILEY-VCH

DOI: 10.1002/ ((please add manuscript number))
**Article type: Full Paper**

# Layer-by-Layer Coating of Aminocellulose and Quorum Quenching Acylase on Silver Nanoparticles Synergistically Eradicate Bacteria and Their Biofilms

*Aleksandra Ivanova, Kristina Ivanova, Antje Tied, Thomas Heinze, and Tzanko Tzanov*[*]

A. Ivanova, Dr. K. Ivanova, Prof. T. Tzanov
Group of Molecular and Industrial Biotechnology
Department of Chemical Engineering
Universitat Politècnica de Catalunya, Rambla
Sant Nebridi 22, 08222, Terrassa, Spain
E-mail: tzanko.tzanov@upc.edu

A. Tied, Prof. T. Heinze
Center of Excellence for Polysaccharide Research
Institute of Organic Chemistry and Macromolecular Chemistry
Friedrich Schiller University of Jena
Humboldtstraße 10, 07743 Jena, Germany

Keywords: acylase, aminocellulose, silver nanoparticles, layer-by-layer, antibacterial and antibiofilm activities

The emergence of antibiotic resistant bacteria and the failure of the existing antibacterial therapeutics call for development of novel treatment strategies. Furthermore, the formation of bacterial biofilms restricts the drugs penetration and efficiency, causing life-threatening infections. Bacterial attachment and biofilm formation are regulated by the cell-to-cell communication phenomenon called quorum sensing (QS). In this work, antimicrobial silver nanoparticles (AgNPs) are decorated in a Layer-by-Layer fashion with the oppositely charged aminocellulose (AM) and acylase to generate hybrid nanoentities with enhanced antibacterial and antibiofilm activities as well as reduced cytotoxicity. Acylase, a quorum quenching enzyme that degrades the QS signals in the extracellular environment of bacteria, disrupts the bacterial QS process and together with the bactericidal AM synergistically lowers 4-fold the

minimum inhibitory concertation of the AgNPs templates towards Gram-negative *Pseudomonas aeruginosa* (*P. aeruginosa*). The hybrid nanoparticles in 8-fold lower concentration than the AgNPs, inhibit 45 % of the QS-regulated virulence factors produced by the reporter *C. violaceum* bacterial strain and reduce by 100 % the *P. aeruginosa* biofilm formation. Moreover, the sequential deposition of antibacterial/antibiofilm active and biocompatible biopolymers onto the AgNPs allows the engineering of safe nanomaterials that do not affect the viability of human cells.

## 1. Introduction

Antimicrobial drug resistance has become a serious public health threat and one of the leading causes of death worldwide.[1] The failure of the existing antibiotic therapies is the reason for the increased mortality and morbidity in hospitals, as well as the huge economic burden.[2] Besides the specific resistant mechanisms, such as i) modification of the drug target, ii) antibiotics degradation and iii) over-expression of efflux pumps for the exportation of antibiotics out of the cell, bacteria are able to express biofilm-specific phenotypes, which are extremely tolerant to the most of the currently available antimicrobials.[3,4] Bacterial biofilms are surface attached community of cells encased in a self-produced polymeric matrix that suppress the host immune response and protect the pathogens from the antimicrobial agents. Biofilm formation begins with bacterial attachment to the host tissues or non-living medical surfaces, which is followed by the production of specific signaling molecules. These signals, specifically recognized by Gram-negative bacteria in the quorum sensing (QS) process, are acyl-homoserine lactones (AHL). QS governs the virulence factors production, biofilm formation and establishment of severe bacterial infections.[5,6] The community-acquired biofilms of bacteria and the appearance of drug resistant strains hinder the effective infection

treatments and therefore calls for the development of new antimicrobial alternatives with lower potential for resistance selection.[7]

The introduction of new antibiotic analogues with similar to the original drug structural and functional characteristics is only a short-term antibacterial strategy, compared to the time and resources consuming development of the next generation antibiotics.[2] In this respect, nanoparticles (NPs) have brought new perspectives for improving the antibacterial efficacy of antibiotics due to the high surface to volume ratio and their unique physical and chemical properties. Nano-formulated antimicrobials have shown enhanced antibacterial activity compared to their bulk counterparts because of the improved interaction with bacterial membrane and easier access to the target site.[8] Furthermore, the nano-form enhances the penetration of the active in the biofilm structure, which is crucial in determining the treatment efficacy of the antimicrobials.[9]

Silver nanoparticles (AgNPs) are one of the most widely exploited nanobactericides in wound dressing materials, medical devices and textiles.[10] Despite their strong antibacterial potential against susceptible and drug-resistant bacteria, the use of AgNPs in medical practice is limited because of their low stability, toxicity and the possibility to invoke resistance in bacteria.[11,12] To address these issues, green nanotechnology approach based on biocompatible compounds, instead of toxic chemicals, has been employed for the synthesis of stable AgNPs with reduced toxicity. Our group has integrated cationic biopolymers, e.g. chitosan and aminocellulose (AM),[13-15] and enzymes, e.g. amylase, with $Ag^0$ into the same hybrid nanosystem to eliminate bacteria and their biofilms, without affecting human cells viability. Amino-bearing biopolymers are membrane-damaging bactericides with high efficiency towards both Gram-positive and Gram-negative bacteria and reduced possibility for resistance development.[16] On the contrary, hydrolytic quorum quenching enzymes (QQE) such as acylase and lactonase that degrade the QS signals in the extracellular environment and disrupt the QS, without killing bacteria,[17,18] have been considered as an innovative tool to render the pathogens less

virulent and more susceptible to lower antibiotic dosage.[19-22] We have applied these QQEs for surface engineering of medical device to inhibit QS and reduce the drug resistant biofilm formation.[23,24]

In this work, the QQE acylase and amino-bearing biopolymer AM were used for the first time for layer-by-layer (LbL) coating of AgNPs templates in order to obtain hybrid enzyme/biopolymer/metal NPs with enhanced antibacterial and antibiofilm activities against the Gram-negative *Pseudomonas aeruginosa*. LbL is a simple and versatile self-assembling technology of oppositely charged molecules used for production of multifunctional nanocoatings[25] on inert macro, micro and nano-sized templates[26] under mild conditions, without the need for any chemical modification.[27] Herein, the coating of antibacterial AgNPs with membrane disrupting biopolymer is expected to create high local positive charge density, which synergistically with the activity of the nano-sized template will improve the interaction of the novel hybrid NPs with bacterial membranes and potentiate the bactericidal activity of AgNPs at lower dosage. Furthermore, the inclusion of acylase in the nano-hybrids will inhibit the establishment of *P. aeruginosa* biofilm, making the pathogen susceptible to low and safe to human cells AgNPs concentrations. The functionality of the novel NPs will be evaluated in terms of QS inhibition potential, antibacterial activity and capacity to prevent and eradicate *P. aerugnosa* biofilms. Finally, the cytotoxicity of the NPs will be assessed *in vitro* towards human fibroblasts cells.

## 2. Results and Discussions

### 2.1. Nanoparticles Characterization

AgNPs were produced and used as an active antibacterial NP-template for LbL self-assembling with amino-bearing AM and anti-QS acylase. The synthesis of AgNPs was carried out in an aqueous solution as previously described.[28] The change from transparent to green-grey colored suspension and the appearance of the absorbance peak at 400 nm confirmed

AgNPs formation (**Figure S1, Supporting Information**). The resulting NPs, with -56,15 mV zeta-potential and 20-25 nm size (**Table S1, Supporting Information**), were then sequentially coated with oppositely charged AM and acylase in an LbL fashion. The positively charged AM was applied as a first layer, changing the AgNPs zeta potential to + 30.8 mV. Subsequently, the deposition of negatively charged QQE acylase switched the NPs surface charge to – 29.97 mV forming stable LbL Ag@AM_AC NPs (**Figure 1B**).

The morphology of the LbL Ag@AM_AC NPs was further assessed using transmission electron microscopy (TEM). TEM images (**Figure 1C, D**) revealed the generation of quasi-spherical in shape NPs with an average size of 30-35 nm, which are embedded in a hybrid macromolecular shell of AM and AC. The data revealed a small size of the NPs (**Figure 1E**). The STEM mapping and energy dispersive x-ray (EDX) spectroscopy of an individual LbL Ag@AM_AC NP further confirmed the presence of elemental silver in the metal NP core (bright central region), as well as carbon and oxygen in the AM and AC shell (**Figure 1F**). The copper ions detected by the EDX (**Figure 1G**) are from the grid used for the analysis.

The activity of acylase in the LbL Ag@AM_AC NPs was further assessed following a colorimetric method and an *in vitro* bioassay with a reporter bacterial strain. In the colorimetric assay, the enzymatic activity of acylase was confirmed via the degradation of N-acetyl-L-methionine substrate to L-methionine and the subsequent development of purple color upon interaction with ninhydrin (**Figure S2, Supporting Information**).[23]

The QQ activity of the enzyme after its deposition onto the AgNPs templates was demonstrated through the degradation of the QS signals in *Chromobacterium violaceum* (*C. violaceum*) CV026. *C. violaceum* CV026 is mini-Tn5 mutant that produces a purple pigment (violacein) upon the addition of AHL signaling molecules.[29] The QQE degrades the AHL signals, consequently inhibiting the violacein production.[30] This Gram-negative bacterium has been used in our group to demonstrate the anti-QS potential of acylase from *Aspergillus melleus*.[23,24] LbL Ag@AM_AC NPs, at sub-inhibitory concentrations ($1.56x10^7$ NPs $mL^{-1}$),

degraded the AHLs and disrupted the QS process, reducing the violacein production by 45 % (**Figure 2**), without affecting *C. violaceum* growth (**Figure S3, Supporting Information**). The same amount of pristine AgNPs, however, did not influence the production of this pigment, confirming the presence of active enzyme on the nano-template, which is able to quench the signals and inhibit the QS-regulated behavior in the Gram-negative pathogen *P. aeruginosa*. Interruption of QS in the extracellular environment is a new approach for attenuation of bacterial virulence and boosting the bactericidal activity of existing antimicrobials at lower dosage.[31] Moreover, the anti-QS based strategy reduces the risk of drug resistance development.

### 2.2. Antibacterial efficiency of AgNPs and LbL Ag@AM_AC NPs

The minimal inhibitory concertation (MIC) of the AgNPs template and the developed LbL Ag@AM_AC NPs was determined against *P. aeruginosa* by a standard broth dilution method.[9] The lowest concentrations, where visible bacterial growth (OD=0) was not observed, were considered as MIC. The stand-alone AgNPs demonstrated antibacterial activity against *P. aeruginosa* at concentration of $1x10^9$ NPs $mL^{-1}$ (**Figure 3**). However, the functionalization of AgNPs with AM enhanced their bactericidal activity by 2-fold, as anticipated on the basis of our previous findings.[27] The nanoscale transformation of amino-bearing polymers enhanced the availability of the positively charged amino groups, resulting in increased interaction with bacterial cells and stronger bactericidal effect than the pristine solution.[32]

Furthermore, the inclusion of QQ acylase improved 4-fold the NPs inhibitory efficacy against *P. aeruginosa* (**Figure 3**). The ability of acylase to interfere with QS in *P. aeruginosa* and attenuate its virulence is thought to potentiate the bactericidal capacity of the actives, lowering their antibacterial effective concentrations. In order to outline the role of the enzyme, the AgNPs template were coated with antibacterial AM and a catalytically inert protein, e.g.

BSA, instead of AC (**Figure S4, Supporting Information**). The obtained control NPs possess similar physicochemical properties (i.e. size, zeta-potential and concentration) as the LbL Ag@AM_AC NPs, but were less active towards *P. aeruginosa*, confirming the synergistic role of acylase and AM in enhancing the antibacterial properties of the AgNPs template. The bactericidal activity of LbL Ag@AM_AC was further confirmed after plating onto selective Cetrimide agar. The LbL Ag@AM_AC NPs completely eliminated the *P. aeruginosa* cells at lower concentrations when compared to the same amount of AgNPs due to the complementary action of the bactericidal nano-sized core and the anti-QS acylase (**Figure S4B, Supporting Information**). Although, our pervious findings have shown that higher number of layers is needed to introduce desired antibacterial functionality on inert NP template, herein the deposition of more AM/acylase layers did not result in enhanced bactericidal activity.[27] In contrary, more layers diminished the effect of the active AgNPs template and no synergy between the nanoform and polymeric AM/acylase was observed (data not shown).

In order to study the physical changes of bacteria upon exposure to LbL Ag@AM_AC NPs, ultrastructural analysis using TEM was performed. A clear difference in the morphology between the treated (**Figure 3B**) and non-treated (**Figure 3C**) *P. aeruginosa* cells was observed. The LbL Ag@AM_AC NPs adsorbed onto the bacterium surface, leading to outer membrane disintegration and cytoplasmic leakage. Moreover, some of the LbL NPs were observed in the cytoplasmic space, indicating their ability to penetrate the membrane and affect essential for bacterial cells life-supporting metabolic processes as cells respiration (**Figure 3C**). It could be anticipated that the novel hybrid NPs kill bacteria via a combination of mechanisms including interaction with bacterial cell wall, reactive oxygen species (ROS) production[33] and modulation of microbial signal transduction pathways.[34] The potential of AgNPs template and LbL Ag@AM_AC NPs to generate ROS and kill *P. aeruginosa* was further investigated. In contrast to the positive control (ROS inducer - bacteria incubated with

2, 2-azobis (2-amidinopropane) dihydrochloride (AAPH), the AgNPs and LbL Ag@AM_AC NPs did not generate ROS similar to the negative control containing only bacteria (**Figure S5, Supporting Information**). Thus, the bactericidal AgNPs and LbL Ag@AM_AC NPs cause cellular death without ROS-related oxidative damage.

### 2.3. Antibiofilm activity

*P. aeruginosa* is an opportunistic Gram-negative pathogen, responsible for variety of difficult to treat infections[35] due to its ability to attach and form robust biofilm structures on medical devices and living tissues, that aggravate the host immune response and resist the antibiotic therapies. *P. aeruginosa* biofilm formation is a complex bacterial mode of growth, which is under the control of QS. [35] In this work, we aimed to develop hybrid NPs that interrupt the QS process via degradation of the AHL signaling molecules and thus effectively inhibit and eliminate the biofilm growing *P. aeruginosa* cells at lower concentrations than the stand alone AgNPs. The antibiofilm activity (biofilm growth inhibition and elimination) of the NPs was studied by crystal violet and Live/dead™ *Bac*Light™ assays to quantify the total biofilm mass and visualise the live and dead cells on a model polystyrene surface.

#### *2.3.1. Inhibition of P. aeruginosa biofilm formation by LbL Ag@AM_AC NPs*

*P. aeruginosa* was cultured in the presence of different concentrations of LbL Ag@AM_AC NPs and AgNPs for 24 h to determine the minimum biofilm inhibitory concentration (MBIC). The MBIC is defined as the concentration at which the total biofilm mass was inhibited by > 90 %, when compared to the control with only bacteria corresponding to 100 % biofilm formation. The MBIC of the NPs decorated with AM and anti-QS enzyme was 8-fold lower ($6.25 \times 10^7$ NPs $mL^{-1}$) than the MBIC of the pristine AgNPs ($1.25 \times 10^8$ NPs $mL^{-1}$) (**Figure 4A**). The obtained microscopic images of *P. aeruginosa* biofilms after 24 h incubation with LbL Ag@AM_AC NPs at the determined MBIC further confirmed their enhanced antibiofilm activity (**Figure 4B**). The LbL Ag@AM_AC NPs at their MBIC completely inhibited the biofilm growth of *P. aeruginosa* observing only few individual cells on the surface. In

contrast, the AgNPs at the same concentration, showed negligible antibiofilm activity and formed typical for the mature biofilm bacterial clusters, similar to the control (only *P. aeruginosa*) (**Figure 4B**). All these results indicated the synergy between the bactericidal nano-sized template and the antibiofilm acylase enzyme. Interrupting the QS process through acylase-catalysed degradation of bacterial signals in the extracellular bacterial space have been shown very effective for inhibiting *P. aeruginosa* virulence and establishment of drug resistant biofilms, without bacteria killing.[36] Herein, the deposition of acylase on the bactericidal AgNPs yielded multifunctional nanoentities able to inhibit the QS-regulated pathological processes and at the same time completely eliminate the biofilm forming bacteria at lower dosage of the bactericidal agent, thus exerting less evolutionary pressure on bacteria for resistance development. The engineered LbL NPs demonstrated high potential for eradicating *P. aeruginosa* and therefore could be exploited in the development of coatings on medically relevant surfaces for preventing biofilm associated infections.

*2.3.2. Elimination of P. aeruginosa biofilms with LbL Ag@AM_AC NPs*

*P. aeruginosa* cells in already established biofilms are enclosed in an extracellular polymeric matrix (EPM), which is the bacterium protective barrier against the action of the immune system and the effective penetration of the conventional drugs.[35] Therefore, the potential of the LbL Ag@AM_AC NPs to overcome the inherent biofilm resistance and penetrate through the *P. aeruginosa* biofilm was further assessed. The minimum biofilm eradication concentration (MBEC) of the LbL Ag@AM_AC NPs, i.e. the lowest NPs concentration at which bacteria fail to re-grow, was determined using crystal violet. The MBEC of the novel NPs was 8-fold lower ($6.25x10^7$ NPs $mL^{-1}$) than the MBEC determined for the stand-alone AgNPs template ($2x10^9$ NPs $mL^{-1}$) **(Figure 5A)**.

Although the anti-QS approaches are considered more relevant in inhibiting the early stage of biofilm formation, rather than acting on already established surface-attached bacterial

communities, several studies have demonstrated the ability of acylase to reduce bacterial biofilms. These findings are in line with the assumption that the QS signaling has an important role for maintaining the integrity of already formed *P. aeruginosa* biofilm.[37-39] In particular, the process is part of the extracellular DNA release and the structural stability of the biofilm.[35] We believe that the nano-formulated acylase weakens and destabilises the protective EPM barrier, enhancing the access of therapeutic NPs to the bacterial cells in the mature biofilm. Moreover, decorating the AgNPs with a cationic polymer adds an additional mechanism for bacteria killing, through membrane disruption, potentiating the antibacterial and antibiofilm activities of AgNPs at lower concentrations.[40,41] Previous results of our group, have demonstrated enhanced antibacterial and biofilm activities of nano-formulated antimicrobials (such as AM, penicillin and vancomycin) in comparison to their bulk counterparts, due to easier penetration into biofilm structures and access to the target bacteria.[42]

The effect of LbL Ag@AM_AC NPs and AgNPs template (at concertation $6.25x10^7$ NPs $mL^{-1}$) on established biofilms was assessed with fluorescence microscopy after Live/Dead staining. A significant decrease in the cell viability and biofilm density (most of the cells were stained in red) was observed, when the 24 h old biofilm was treated with LbL Ag@AM_AC NPs (**Figure 5B**). In contrast, the application of unmodified AgNPs resulted in reduced cells viability, however, without any significant decrease/elimination of the total biofilm mass (**Figure 5B**). Therefore, the novel LbL Ag@AM_AC NPs possess great therapeutic potential and could be employed in the design of topical formulations for treatment of severe skin infections or for coating of medical devices and surfaces in contact with humans.

### 2.4. Biocompatibility assessment

AgNPs are known antibacterial agent widely used as disinfectant or coating of medically relevant surfaces,[43] however their biocompatibility is an important issue to be considered for

biomedical application. Therefore, the viability of human cells upon exposure to AgNPs template and LbL-decorated NPs at their bactericidal concentrations was assessed after 24 h of incubation. AgNPs demonstrated high toxicity and reduced by 20 % the viability of human cell (**Figure 6A**), while nearly 100 % of the skin cell fibroblasts were viable in the presence of functionalised with AM and acylase AgNPs (**Figure 6A**). Unlike the AgNPs, the LbL Ag@AM_AC NPs did not cause cell morphology changes compared to the negative control (**Figure 6B**). The toxicity of AgNPs greatly depends on their concentration, size, shape, surface chemistry/coating and dissolved silver ions from the NPs.[44] Here, to benefit from the outstanding performance of AgNPs in terms of microbial elimination and at the same time minimise their toxicity, we engineered in a "safe by design" approach novel biomaterial-coated AgNPs. Functionalisation of the AgNPs with biocompatible and antibacterial polymers and enzymes is a promising strategy to change the AgNPs toxicity profile and boost their bactericidal properties.[44]

## 3. Conclusion

In this work, AgNPs were LbL coated with antimicrobial AM and QQ acylase in order to generate safe and highly efficient antibacterial and antibiofilm hybrid nano-entities. The bilayered decoration of AgNPs template resulted in 4-fold enhanced bactericidal activity towards the Gram-negative *P. aeruginosa* due to the synergy between the metal core and the nanoformulated antibacterial AM and antibiofilm acylase. Moreover, these hybrid NPs were able to degrade the AHL signaling molecules of Gram-negative bacteria, inhibiting the QS regulated biofilm formation by *P. aeruginosa* at lower concentrations than the pristine AgNPs. The anti-QS acylase has also affected the pathogenicity and the integrity of already established *P. aeruginosa* biofilm, increasing the bacterium susceptibility to antibacterial AgNPs. LbL building of a biocompatible shell of AM and acylase around the AgNPs is a

safe-by-design approach for development of metal-based nanoantimicrobials with decreased toxicity to mammalian cells and improved efficacy. The combination of membrane-disrupting AM and QQ acylase on the AgNPs surface provides an innovative tool for treatment of bacterial infections, at minor risk for resistance development.

## 4. Experimental Section

*Materials:* Microcrystalline cellulose (Avicel PH-101 from Fluka) was used for the preparation of the 6-deoxy-6-(ω-aminoethyl) aminocellulose (AM) derivative as previously described.[27] Acylase from *Aspergillus melleus* (E.C 3.5.1.14; 4.5 % (w/w) protein content and 2.49 U $mg^{-1}$ specific activity, pI =2.3) was purchased from Sigma-Aldrich (Spain). *P. aeruginosa* bacterium (ATCC® 10145™) and the human foreskin fibroblast cells (ATCC® CRL-4001™, BJ-5ta) were obtained from American Type Culture Collection (ATCC LGC Standards, Spain). AlamarBlue® cell viability reagent was purchased from Invitrogen, Life Technologies Corporation (Spain). Ultrapure water (MilliQ® plus system, Millipore) with 18.2 MΩ.cm resistivity was used in all experiments. All other chemical and microbiological reagents were purchased from Sigma–Aldrich unless otherwise specified.

*Silver NPs synthesis:* Single step citrate reduction reaction was employed for the preparation of AgNPs. The glassware used for AgNPs synthesis was thoroughly washed with aqua regia (HCl and $HNO_3$ in 3:1). Silver nitrate (0.02 % $AgNO_3$ w/v) was dissolved in 100 mL deionized water and boiled at 150 °C under continuous stirring. 2 mL of sodium citrate solution (1 % $Na_3C_6H_5O_7$ in deionized water) were added to the silver nitrate solution dropwise. Then, the solution was left for ~ 30-40 min at 150 °C with stirring.

*LbL coating of AgNPs with aminocellulose and acylase:* Negatively charged AgNPs were used as colloidal templates for LbL deposition of the positively charged AM and negatively charged acylase. AgNPs were diluted (2x) in mQ water and the pH was adjusted to 8. The deposition of each oppositely charged layer onto the AgNPs template was carried out by

mixing 7.35 mL of the diluted AgNPs with 0.65 mL of 10 mg $mL^{-1}$ of AM (in mQ water) deposited as a first layer, and acylase (in 100 $m_M$ Tricine buffer, pH 8) as a second layer. The samples were agitated for 5 min and were left for 1 h at room temperature. After the AM deposition, the NPs were ultracentrifuged at 18 000 rpm for 50 min, while after the acylase deposition the centrifugation was carried out for 15 min at 15 000 rpm. Finally, the pellets of LbL Ag@AM_AC NPs were collected and resuspended in 1 mL mQ water. In order to outline the role of acylase in the hybrid nanoentities, we further developed control NPs decorated with non-catalytically active bovine serum albumin (10 mg $mL^{-1}$ BSA), instead of QQ acylase. These samples (LbL Ag@AM_BSA NPs) were used as a control in the antibacterial test.

*Nanoparticles characterization:* Spectrophotometric measurements were performed in a microplate reader Infinite M200, Tecan (Austria). The UV–vis spectra were collected in the range of 300–600 nm, recording absorbance at a 2 nm step. TEM and dynamic light scattering was used to determine the size and the zeta-potential of the Ag NPs.

The successful buildup of the LbL constructs was studied by measuring the variation of zeta-potential of the NPs after each layer deposition using a Zetasizer Nano Z (Malvern Instruments Inc., U.K.). After the LbL assembly, the size and concentration of the NPs was assessed by Nanoparticle Tracking Analyzer (NTA) (NanoSight LM10, Malvern Instruments Inc., U.K.) equipped with LM10 Laser 405 nm NP viewing unit and sCMOS camera. Software NTA 3.2 Dev Build 3.2.16 was used to capture several frames of the NP suspension to obtain the size of particles and their final concentration. The reported average particle size represents the mean values ± standard deviations of five measurements per sample. The size and morphology of the LbL NPs were also examined by TEM using a TEM JEOL 1010 equipped with a camera CCD Orius (GATAN) at an operating voltage of 80 kV. The sample was prepared by dropping the NP solution on carbon-coated grids.

*Enzymatic activity:* The enzyme activity of LbL Ag@AM_AC NPs was evaluated by a colorimetric assay using N-acetyl-L-methionine (NAMET) as a substrate and in a bioassay using *C. violaceum* CECT 5999. In the colorimetric assay, 200 µL of tricine buffer (100 $m_M$, pH 8.0) and 200 µL of 0.5 $m_M$ cobalt chloride solution were added to 200 µL samples and equilibrated at 37 °C. Then, 200 µL of 100 $m_M$ NAMET in tricine buffer (100 $m_M$, pH 8.0) were added, and the test tubes were incubated for 30 min. The reaction was stopped by rising the temperature to 100 °C for 4 min. The product of the enzymatic reaction was determined using the ninhydrin assay as follows: 200 µL of the sample was mixed with 400 µL of 2 % (w/v) ninhydrin solution (prepared in 200 $m_M$ citrate buffer, pH 5 and ethylene glycol monomethyl ether (1:1)) and 20 µL 1.6 % (w/v) stannous chloride solution. The samples were incubated for 20 min at 100 °C and cooled down before measuring their absorbance at 570 nm. Non-coated AgNPs were used as a control in all the experiments.

*Quorum quenching activity: C. violaceum* CECT 5999 was used to test the QQ activity of acylase and its ability to interfere with the QS process through the degradation of C6-HSLs, as previously described.[24] *C. violaceum* CECT 5999 is a mutant bacterial strain that in the presence of AHLs produces the purple pigment violacein. Briefly, the bacterium was grown on Luria Bertani broth (LB) agar (supplemented with 25 µg $mL^{-1}$ kanamycin (Sigma-Aldrich)), and the plates were incubated at 26 °C for 48 h. Afterwards, the bacterium was inoculated in LB medium supplemented with 25 µg $mL^{-1}$ kanamycin at 26 °C for 12-16 h. For the bioassay, *C. violaceum* was diluted to optical density 0.004 ($OD_{660}$) in fresh medium supplemented with 25 µg $mL^{-1}$ kanamycin and 5 $\mu_M$ AHLs (C6-HSL). Then, 350 µL of the inoculum were mixed with 350 µL of LbL Ag@AM_AC NPs and uncoated AgNPs template at their subinhibitory concentrations, and the samples were left at 26 °C overnight with 550 rpm shaking. Bacterium without NPs was used as a control. After the time of incubation, 200 µL of each sample were transferred in 2 mL Eppendorf, mixed with 200 µL of 10 % sodium dodecyl sulfate and vortexed for 5 s. Following that, 500 µL of 1- butanol were added for the

violacein extraction and the samples were centrifuged for 5 min at 13, 000 rpm. The butanol phase containing violacein was collected and the absorbance was measured at 584 nm.

*Minimal inhibitory concentration determination:* The MIC and MBC of AgNPs and LbL Ag@AM_AC NPs were assessed towards the Gram-negative *P. aeruginosa*. Briefly, bacteria were grown overnight at 37 °C in Mueller Hinton Broth (MHB) medium. Subsequently, 50 µL of different concentration of AgNPs and LbL Ag@AM_AC NPs were mixed with 50 µL bacterial inoculum in MHB (optical density ($OD_{600}$ = 0.01), ~ $10^5$–$10^6$ colony forming units per mL (CFU $mL^{-1}$)) in a 96-well polypropylene microplate and incubated at 37 ºC for 24 h. Subsequently, the *P. aeruginosa* growth in presence of NPs was assessed measuring the OD at 600 nm in a microplate reader (Infinite M200, Tecan, Austria). The samples, where no turbidity (no bacteria growth) was observed ($OD_{600}$ ~0) were considered antibacterial. Afterwards, the NPs bactericidal activity was proven by culturing the samples onto selective agar and incubating the plates for 16 h at 37 °C.

*Transmission Electron Microscopy of Bacterial Samples:* LbL Ag@AM_AC NPs were incubated with *P. aeruginosa* ($OD_{600}$ = 0.01, ~ $10^5$–$10^6$ CFU $mL^{-1}$) for 3h at 37 ºC with shaking. Afterwards, the samples were centrifuged at 4000 g for 5 min and resuspended in fresh fixative solution containing 2.5 % glutaraldehyde and 2 % paraformaldehyde 0.1M phosphate buffer, pH 7.4. The samples were incubated for overnight at 4 °C, washed three times with 0.1M phosphate buffer, pH 7.4 and fixed in 1% osmium tetraoxide. Then, the cells were stained with 2% uranyl acetate, dehydrated in an ethanol, and embedded in Spurr resin. Ultrathin sections were obtained with an Ultracut E (Reichert-Jung) ultramicrotome and counterstained with lead citrate. The slices were deposited on bare mesh copper grids and the sections were observed using JEOL 1100 transmission electron microscope at 80 kV.

*Determination of reactive oxygen species:* 2,7-dichlorodihydrofluorescein diacetate (DCFDA) assay was used to quantitatively measurement of ROS produced in the bacterial cells. Briefly, the bacteria was grown overnight in MHB and was centrifuged at 4000 g for 15 min and

subsequently washed in phosphate buffered saline (PBS). Then, the bacterial cells(optical density ($OD_{600}$ = 0.01), ~ $10^5$–$10^6$ colony forming units per mL (CFU $mL^{-1}$)) were resuspended in PBS and were treated AgNPs and LbL Ag@AM_AC NPs with different concentrations for 3 h at 37 ºC at 230 rpm . Then, 25 µL of 100 $\mu_M$ DCFH-DA were added to the samples and the fluorescence was measured at Ex/Em = 485/535 nm. AAPH was used as a positive control.

*Biofilm Inhibition Test:* The antibiofilm activity of the AgNPs and LbL Ag@AM_AC NPs against Gram-negative *P. aeruginosa* was evaluated using colorimetric crystal violet and Live/Dead assays. Briefly, 50 µL of the NPs and 50 µL of bacteria in tryptic soy broth (TSB) ($OD_{600}$ = 0.01) were placed in a 96-well microplate. The microplate was then incubated for 24 h at 37 °C under static conditions to allow bacteria to form biofilm. After the incubation, the non-adhered bacterial cells were washed three times with 200 µL distilled $H_2O$. The microplate was incubated for 60 min at 60 °C for biofilm fixation. The total biomass was determined using crystal violet assay. The biofilm was stained for 5−10 min with 200 µL of 0.1 % (w/v) crystal violet solution, washed three times with distilled $H_2O$, and dried at 60 °C. Next, 200 µL of 30 % (v/v) acetic acid were added to dissolve the crystal violet and the plate was incubated for 15 min at room temperature. After that, 125 µL of each well were transferred to a new 96-well microplate, and the absorbance was measured at 595 nm. The amount of the dye is directly proportional to the total biomass on the surface, including bacteria cells and the extracellular matrix. Gentamicin (100 µg $mL^{-1}$) was used as a positive control (biofilm inhibition).

The live and dead bacteria into the biofilms were further observed with fluorescence microscopy using Live/dead™ *Bac*Light™ kit, which is comprised of the two nucleic acid fluorescent dyes, SYTO9 and propidium iodide (PI). After the incubation, the non-adhered bacterial cells were washed three times with 200 µL sterile PBS and the microplate was

incubated with 20 µL of SYTO9 and PI in ratio 1:1. After 15 min of incubation in a dark, the samples were visualised under fluorescence microscopy using 20x objective lens. The live cells were stained in green and the dead ones in red.

*Biofilm Eradication assay:* The effect of the NPs on the already established *P. aeruginosa* biofilm was studied using crystal violet and Live/Dead assays. 100 µL of bacteria in TSB ($OD_{600}$ = 0.01) were placed 96-well microplate and the biofilm was allowed to form for 24 h at 37 °C under static conditions and the planktonic cells were washed with sterile PBS. 60 µL of NPs and 60 µL of TSB were placed in the 96-well microplate, subsequently left for 24 h at 37 °C under static conditions. After the incubation, the non-adhered bacterial cells were washed three times with 200 µL sterile PBS. For determination of the total biofilm mass the biofilms were left for fixation for 1 h at 60 °C. Then, the formed biofilms were stained with crystal violet (0.1 % w/v) and dried at 60 °C and further dissolved using 30 % (v/v) acetic acid. 125 µL were transferred into 96-well microplate and the absorbance was recorded at 595 nm. The live and dead bacteria were observed using fluorescence microscopy (20x objective lens) after incubation with 20 µL of SYTO9 and PI in ratio 1:1.

*Biocompatibility of the NPs:* The cytotoxicity of the developed LbL coated AgNPs towards mammalian cells was evaluated using human fibroblast cell line BJ-5ta. The LbL Ag@AM_AC NPs were placed in contact with the previously seeded cells and after 24 h the number of viable cells was quantified using Alamar Blue assay (AlamarBlue®, Invitrogen) as described previously.[8,45] All results are reported as mean values ± standard deviations (n = 3).

**Supporting Information**

Supporting Information is available from the Wiley Online Library or from the author.

**Acknowledgements**

This work was supported by the European project PROTECT "Pre-commercial lines for the production of surface nanostructured antimicrobial and antibiofilm textiles, medical devices, and water treatment membranes" (H2020- 720851). A.I. acknowledges the Ph.D. grant (2019FI_B2 00077) provided by the Generalitat de Catalunya. The authors would like to thank the European Regional Development Fund (FEDER).

**Notes**

The authors declare no competing financial interest.

Received: ((will be filled in by the editorial staff))

Revised: ((will be filled in by the editorial staff))

Published online: ((will be filled in by the editorial staff))

**References**


[1] D. K. Byarugaba, *Int. J. Antimicrob. Agents* **2004**, *24*, 105–110.

[2] L. M. Mahieu, N. Buitenweg, P. Beutels, J. J. De Dooy, *J. Hosp. Infect.* **2001**, *47*, 223–229.

[3] D. Davies, *Nat. Rev. Drug Discov.* **2003**, *2*, 114–122.

[4] G. Feng, Y. Cheng, S.-Y. Wang, D. A. Borca-Tasciuc, R. W. Worobo, and C. I. Moraru, *npj Biofilms Microbiomes* **2015**, *1*, 15022.

[5] P. Fernandes, *Nat. Biotechnol.* **2006**, *24*, 1497–1503.

[6] C. M. Waters, B. L. Bassler, *Annu. Rev. Cell Dev. Biol.* **2005**, *21*, 319–346.

[7] N. Høiby, T. Bjarnsholt, M. Givskov, S. Molin, O. Ciofu, *Int. J. Antimicrob. Agents* **2010**, *35*, 322–332.

[8] M. M. Fernandes, K. Ivanova, A. Francesko, D. Rivera, J. Torrent-Burguès, A. Gedanken, E. Mendonza, T. Tzanov, *Nanomedicine Nanotechnology, Biol. Med.* **2016**, *12*, 2061–2069.

[9] M. M. Fernandes, K. Ivanova, J. Hoyo, S. Pérez-Rafael, A. Francesko, and T. Tzanov, *ACS Appl. Mater. Interfaces* **2017**, *9*, 15022−15030.

[10] A. P. Richter, J. S. Brown, B. Bharti, A. Wang, S. Gangwal, K. Houck, E. A. Hubal, V. N. Paunov, S. D. Stoyanov, O. D. Velev, *Nat. Nanotechnol.* **2015**, *10*, 817–823,.

[11] B. Ramalingam, T. Parandhaman, S. K. Das, *ACS Appl. Mater. Interfaces* **2016**, *8*, 4963–4976.

[12] A. Panáček, L. Kvítek, M. Smékalová, R. Večeřová, M. Kolář, M. Röderová, F. Dyčka, M. Šebela, R. Prucek, O. Tomanec, R. Zbořil, *Nat. Nanotechnol.* **2018**, *13*, 65–71.

[13] A. Francesko, M. Cano Fossas, P. Petkova, M. M. Fernandes, E. Mendoza, and T. Tzanov, *J. Appl. Polym. Sci.* **2017**, *134*, 1–8.

[14] A. Francesko, L. Blandón, M. Vázquez, P. Petkova, J. Morató, A. Pfeifer, T. Heinze, E. Mendoza, T. Tzanov, *ACS Appl. Mater. Interfaces* **2015**, *7*, 9792–9799.

[15] G. Ferreres, A. Bassegoda, J. Hoyo, J. Torrent-burgue, T. Tzanov, *ACS Appl. Mater. Interfaces* **2018**, *10*, 40434−40442.

[16] D. J. Phillips, J. Harrison, S. J. Richards, D. E. Mitchell, E. Tichauer, A. T. M. Hubbard, C. Guy, I. Hands-Portman, E. Fullam, M. I. Gibson, M. I, *Biomacromolecules* **2017**, *18*, 1592–1599.

[17] H. Lade, D. Paul, J. H. yang Kweon, *Int. J. Biol. Sci.* **2014**, *10*, 550–565.

[18] Y. H. Lin, J. L.Xu, J. Hu, L. H. Wang, S. Leong Ong, J. Renton Leadbetter, L. H. Zhang, *Mol. Microbiol.* **2003**, *47*, 849–860.

[19] M. Whiteley, S. P. Diggle, E. P. Greenberg, *Nat. Publ. Gr.* **2017**, *551*, 313–320.

[20] D. Kuo, G. Yu, W. Hoch, D. Gabay, L. Long, M. Ghannoum, N. Nagy, C. V. Harding, R. Viswanathan, M. Shoham, *Antimicrob. Agents Chemother.* **2015**, *59*, 1512–1518.

[21] G. Brackman, P. Cos, L. Maes, H. J. Nelis, T. Coenye, *Antimicrob. Agents Chemother.* **2011**, *55*, 2655–2661.

[22] G. Brackman, K. Breyne, R. De Rycke, A. Vermote, F. Van Nieuwerburgh, *Nat. Publ. Gr.* **2016**, *6*, 20321.

[23] K. Ivanova, M. M. Fernandes, E. Mendoza, T. Tzanov, *Appl. Microbiol. Biotechnol.* **2015**, *99*, 4373–4385.

[24] K. Ivanova, M. M. Fernandes, A. Francesko, E. Mendoza, J. Guezguez, M. Burnet, T.

Tzanov, *ACS Appl. Mater. Interfaces* **2015**, *7*, 27066–27077.

[25] S. Zhao, F. Caruso, L. Dähne, G. Decher, B. G. De Geest, J. Fan, N. Feliu, Y. Gogotsi, P. T. Hammond, M. C. Hersam, A. Khademhosseini, N. Kotov, S. Leporatti, Y. Li, F. Lisdat, L. M. Liz-Marzán, S. Moya, P. Mulvaney, A. L. Rogach, S. Roy, D. G. Shchukin, A. G. Skirtach, M. M. Stevens, G. B. Sukhorukov, P. S. Weiss, Z. Yue, D. Zhu, W. J. Parak, *ACS Nano* **2019**, *13*, 6151–6169.

[26] M. Keeney, X. Y. Jiang, M. Yamane, M. Lee, S. Goodman, F. Yang, *J. Mater. Chem. B* **2015**, *3*, 8757–8770,.

[27] A. Ivanova, K. Ivanova, J. Hoyo, T. Heinze, S. Sanchez-Gomez, T. Tzanov, *ACS Appl. Mater. Interfaces* **2018**, *10*, 3314–3323.

[28] P. C. Lee, D. Melsel, *J. Phys. Chem.* **1982**, *173*, 3391–3395.

[29] L. Steindler, V. Venturi, *FEMS Microbiol Lett* **2007**, *266*, 1–9.

[30] Z. U. Rehman, T. Leiknes, *Front. Microbiol.* **2018**, *9*, 1–13.

[31] M. Lekshmi, A. Parvathi, S. Kumar, M. F. Varela, In *Biotechnological Applications of Quorum Sensing Inhibitors*, (Ed. V. C. Kalia), Springer, Singapore, **2018**, pp. 127–142

[32] M. M. Fernandes, A. Francesko, J. Torrent-Burgués, F. J. Carrión-Fité, T. Heinze, T. Tzanov, *Biomacromolecules* **2014**, *15*, 1365–1374.

[33] S. Dwivedi, R. Wahab, F. Khan, Y. K. Mishra, J. Musarrat, A. A. Al-khedhairy, *PLoS ONE* **2014**, *9*, 1–9.

[34] S. G. Ali, M. A. Ansari, H. M. Khan, M. Jalal, A. A. Mahdi, S. S. Cameotra, *BioNanoScience* **2018**, *8*, 544–553.

[35] T. Rasamiravaka, Q. Labtani, P. Duez, M. El Jaziri, *Biomed Res. Int* **2015**., *2015*,1–17.

[36] A. Ivanova, K. Ivanova, T. Tzanov, In *Biotechnological Applications of Quorum Sensing Inhibitors*, (Ed. V. C. Kalia), Springer, Singapore, **2018**, pp. 3–21.

[37] M. E. Shirtliff, J. T. Mader, A. K. Camper, *Chem. Biol.* **2002**, *9*, 859–871.

[38] D. Paul, Y. S. Kim, K. Ponnusamy, J. H. Kweon, *Environ. Eng. Sci.* **2009**, *26*,1319-1324.

[39] J. Y. Chow, Y. Yang, S. B. Tay, K. L. Chua, W. S. Yew, *Antimicrob. Agents Chemother*. **2014**, *58*, 1802–1805.

[40] K. Giri, L. R.Yepes, B. Duncan, P. K. Parameswaran, B. Yan, Y. Jiang, M. Bilska, D. M. Moyano, M. Thompson, V. M. Rotello, Y. S. Prakash, *RSC Adv.* **2015**, *5*, 105551–105559.

[41] M. Venkatesh, V. A. Barathi, E. T. L. Goh, R. Anggara, M. H. U. T. Fazil, A. J. Y. Ng, S. Harini, T. T. Aung, S. J. Fox, S. Liu, L. Yang, T. M. S. Barkham, X. J. Loh, N. K. Verma, R. W. Beuerman, R. Lakshminarayanana, *Antimicrob Agents Chemother* **2017**, *61*, 1–15.

[42] R. Y. Pelgrift, A. J. Friedman, *Adv. Drug Deliv. Rev* **2013**, *65*, 1803–1815.

[43] M. Akter, T. Sikder, M. Rahman, A. K. M. A. Ullah, K. Fatima, K. F. B. Hossain, S. Banik, T. Hosokawa, T. Saito, M. Kurasaki, *J. Adv. Res.*, **2017**, *9*, 1–16.

[44] B. Das, S. Tripathy, J. Adhikary, S. Chattopadhyay, D. Mandal, S. K. Dash, S. Das, A. Dey, S. K. Dey, D. Das, S. Roy, *J. Biol. Inorg. Chem.* **2017**, *22*, 893–918,.

[45] M. M. Fernandes, A. Francesko, J. Torrent-Burgués, F. J. Carrión-Fité, T. Heinze, T. Tzanov, *Biomacromolecules* **2014**, *15*, 1365–1374.

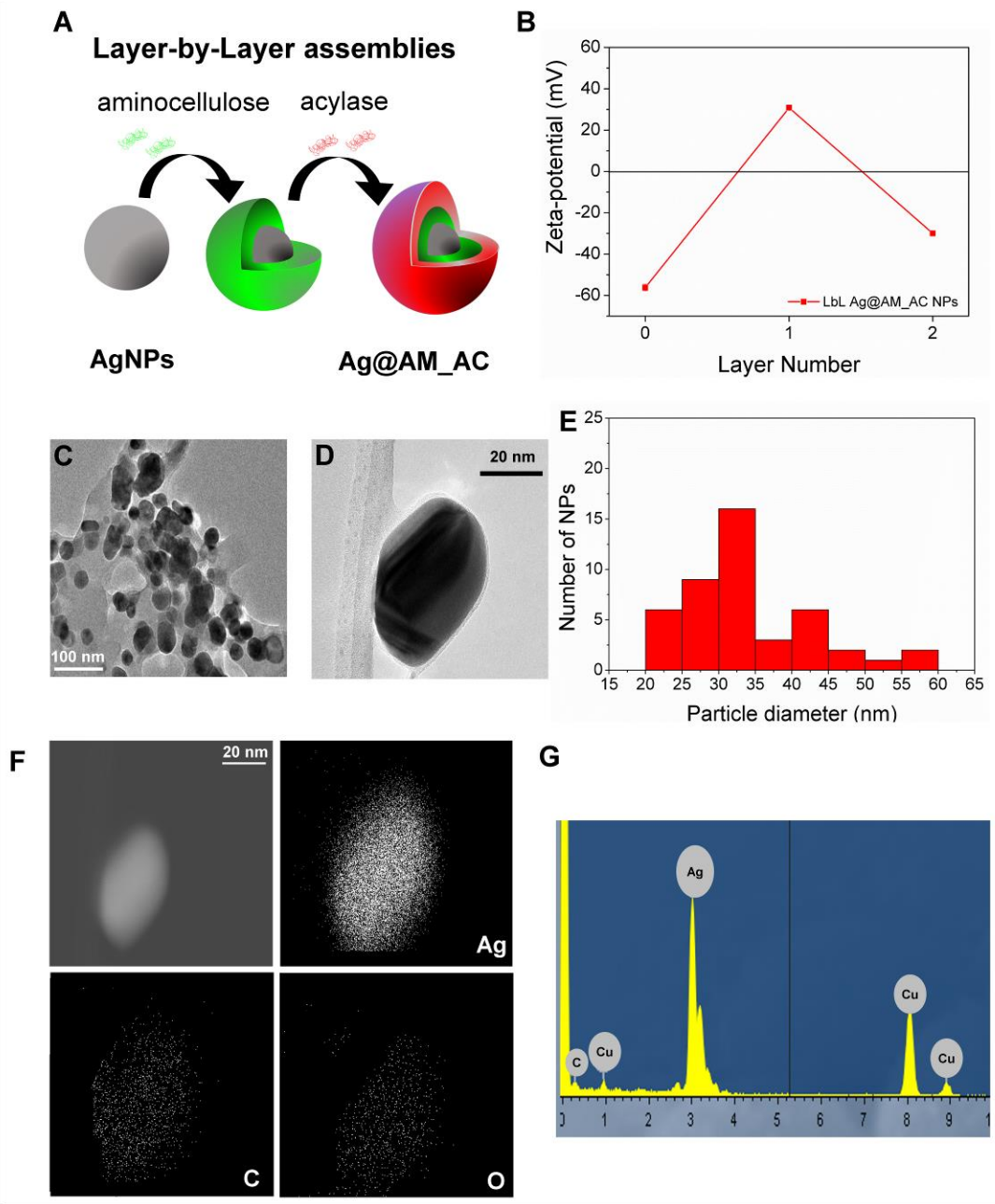


**Figure 1.** LbL Ag@AM_AC NPs preparation and characterization. A) Schematic representation of AgNPs template coating with AM and AC using LbL approach. (B) Zeta-potential of the NPs after each layer deposition. C, D) TEM images of LbL Ag@AM_AC NPs at different magnifications. E) Histogram of LbL Ag@AM_AC NPs size distribution based on the total count using ImageJ software. F) Elemental mapping image and G) STEM-EDX spectrum of an individual LbL Ag@AM_AC NP.

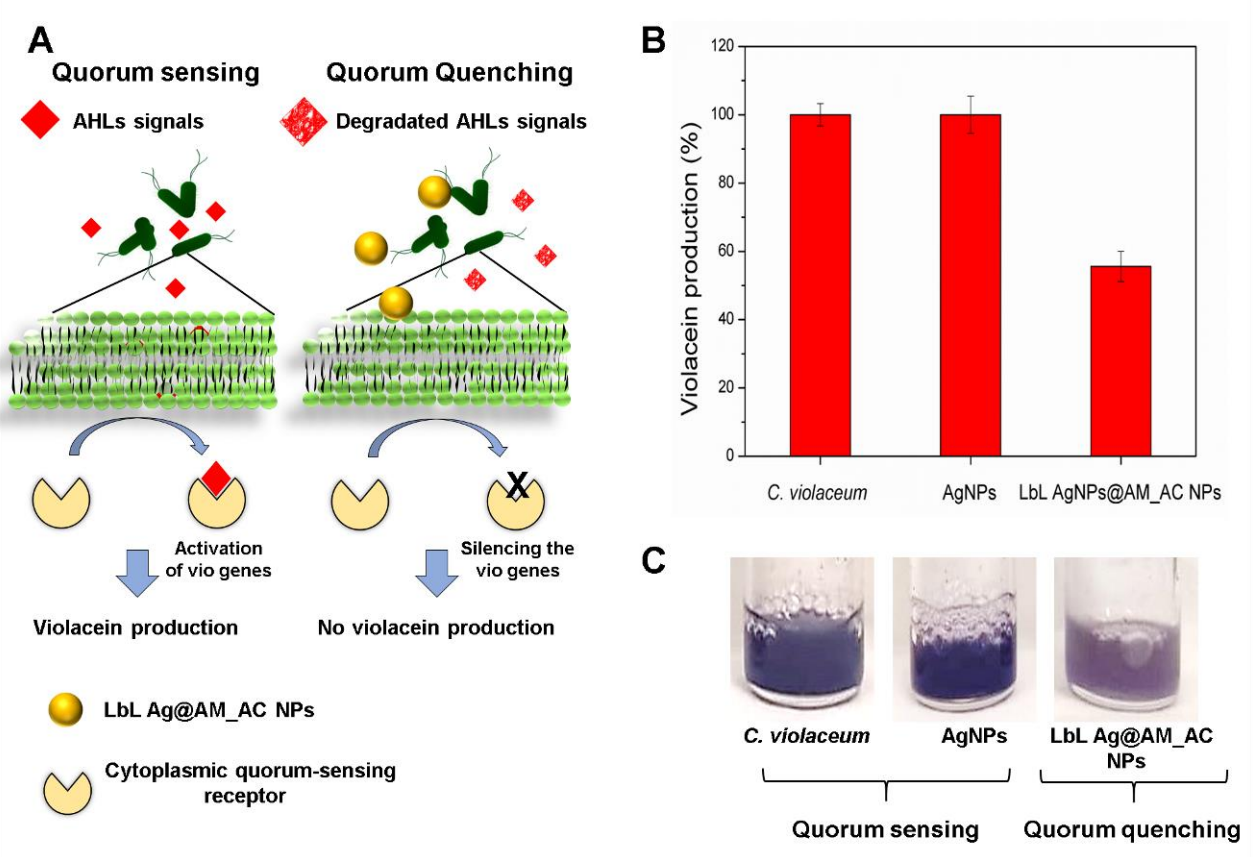


**Figure 2.** Violacein production by *C. violaceum*. A) The AHL signals bind to the cytoplasmic QS receptor and switches on the *vio* genes, activating the violacein production (left). The presence of QQ active NPs breaks down the AHL signals, silencing the expression of the *vio* genes, subsequently inhibiting the violacein production (right). B) Quantification of QS regulated violacein production (%) by *C. violaceum* and C) Representative images of violacein production in presence of AgNPs and LbL Ag@AM_AC NPs.

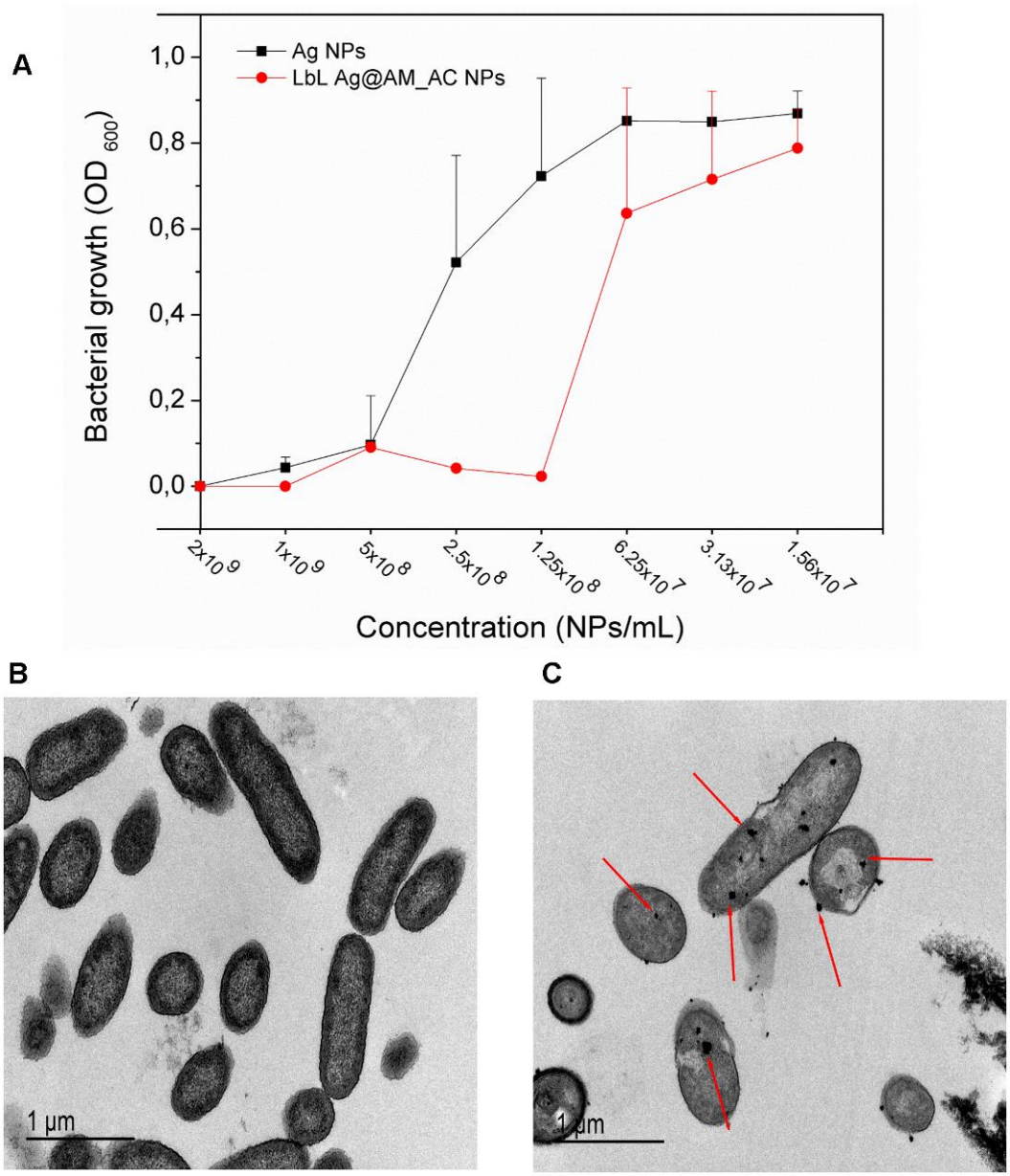


**Figure 3.** A) *P. aeruginosa* growth after 24 h incubation with AgNP template and LbL Ag@AM_AC NPs at different concentrations. TEM images of *P. aeruginosa* before B) and after C) exposure to LbL Ag@AM_AC NPs.

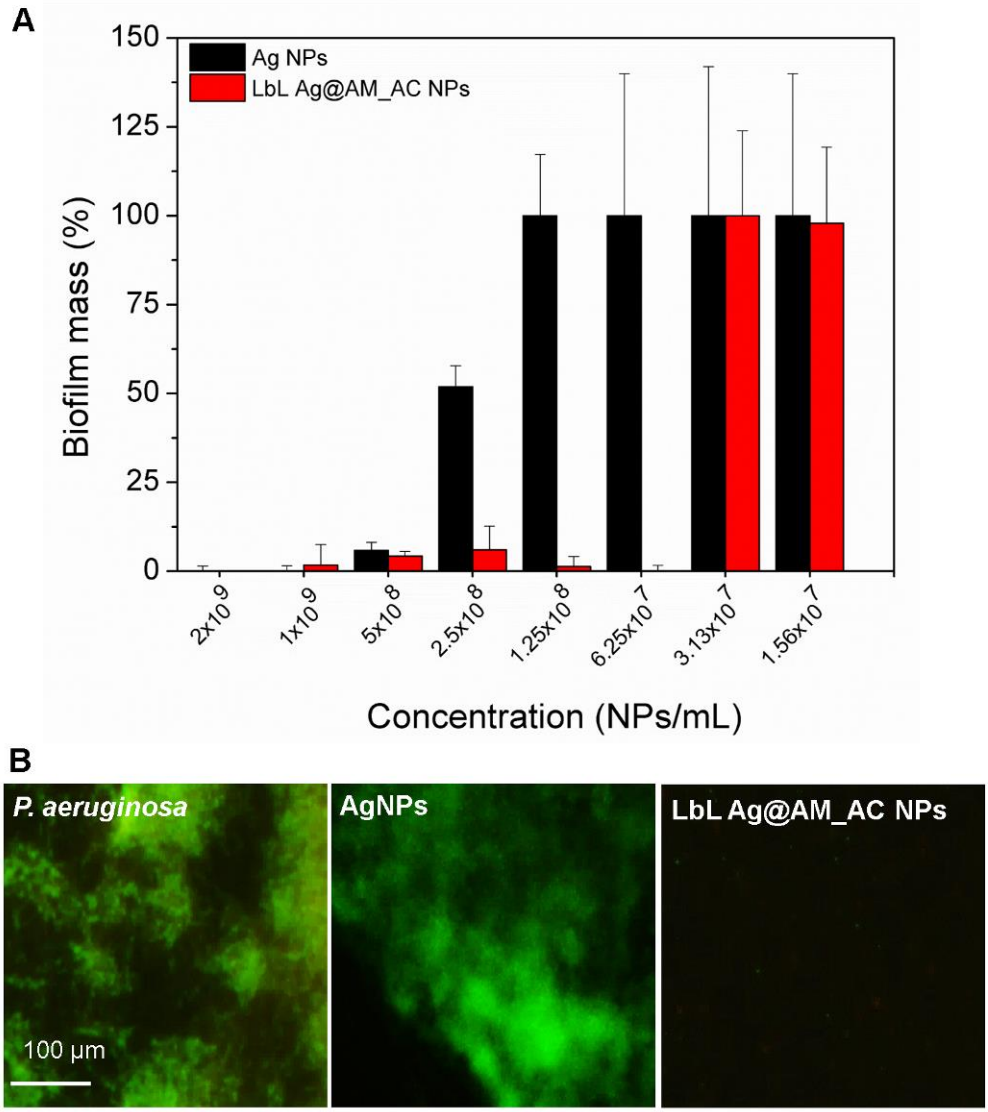


**Figure 4.** *P. aeruginosa* biofilm inhibition. A) MBIC determination of the NPs using crystal violet assay. B) Live/dead™ *Bac*Light™ kit microscopic visualization. The green and red fluorescence images are overlaid. Nonviable bacteria are stained in red, while the viable bacteria appear green.

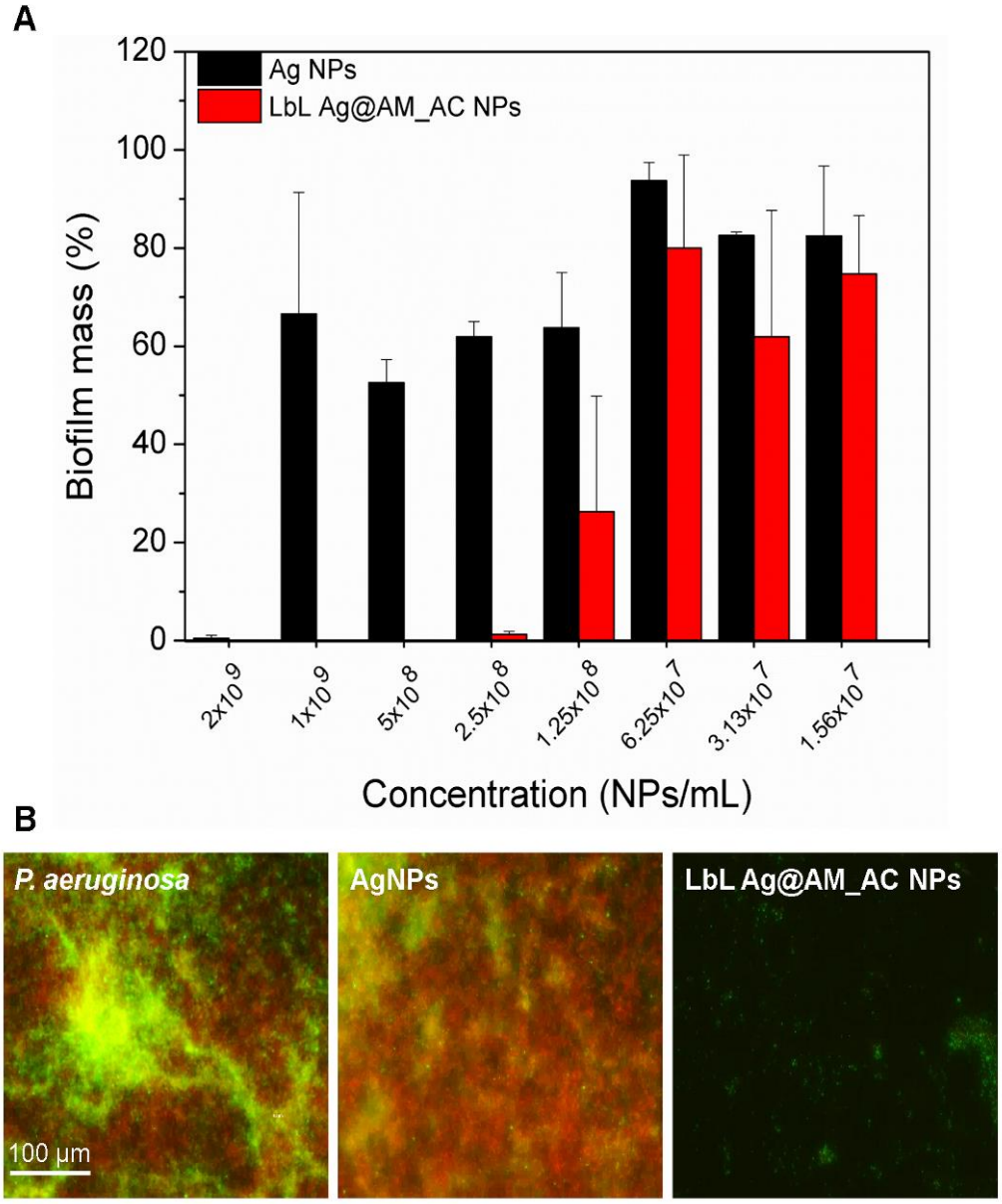


**Figure 5.** Elimination of 24h grown *P. aeruginosa* biofilm. A) MBEC determination of the NPs using crystal violet assay. B) Live/dead™ *Bac*Light™ kit microscopic visualization of *P. aeruginosa* biofilm after 24 h treatment with AgNPs and LbL Ag@AM_AC NPs at the same concentration ($6.25x10^7$ NPs $mL^{-1}$). The green and red fluorescence images are overlaid. Nonviable bacteria are stained in red, while the viable bacteria appear green.

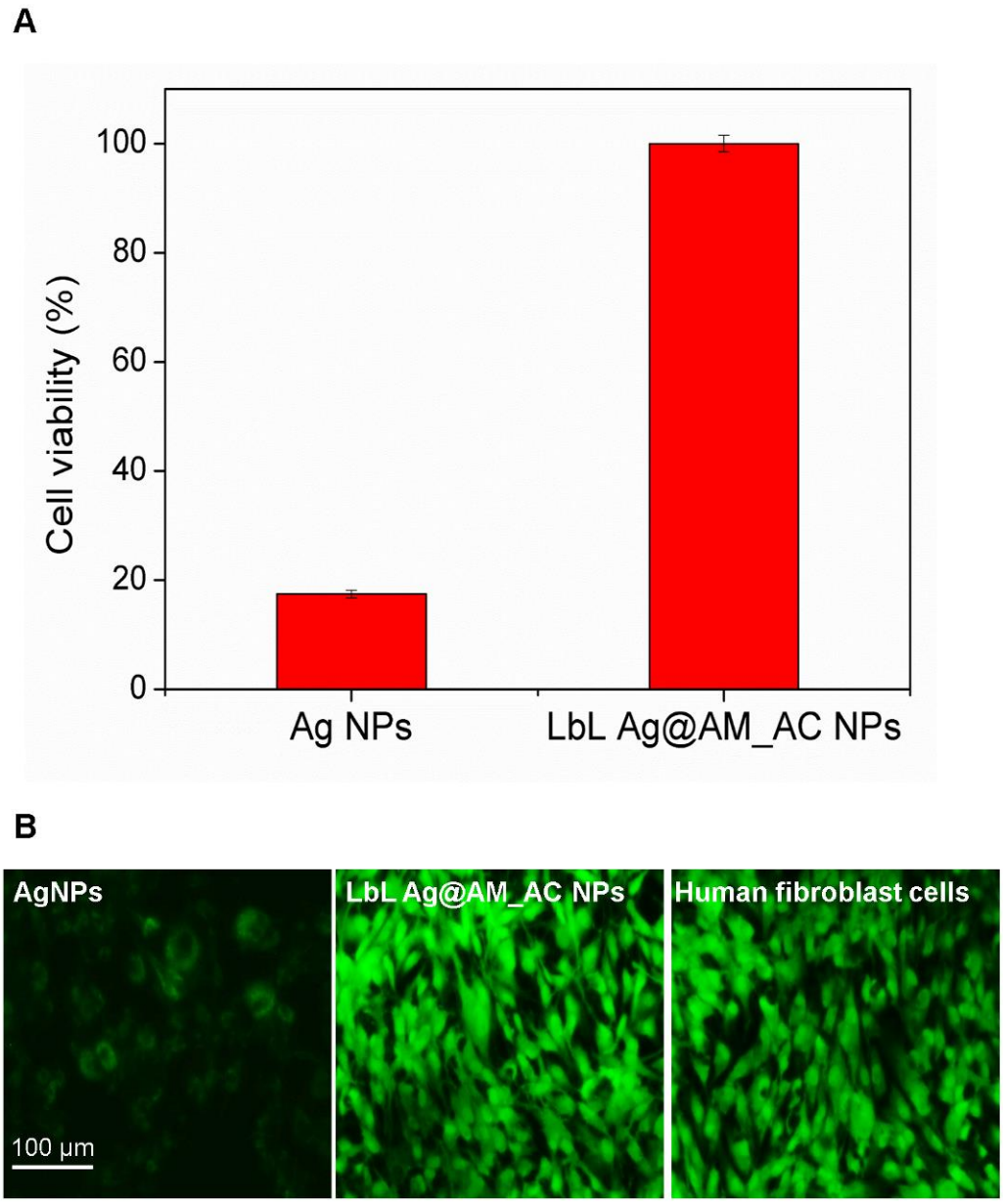


**Figure 6.** Cytotoxicity evaluation. A) Viability (%) of human fibroblasts exposed to AgNPs and LbL Ag@AM_AC NPs after 24 h of incubation assessed by the AlamarBlue assay. B) Live/Dead assay of human fibroblasts after 24 h exposure to AgNPs and LbL Ag@AM_AC NPs. The green and red fluorescence images are overlaid.

**Antimicrobial silver nanoparticles (AgNPs) are decorated in a Layer-by-Layer fashion with toppositely charged aminocellulose (AM) and acylase to generate hybrid nanoentities with enhanced antibacterial and antibiofilm activities as well as reduced cytotoxicity.** The hybrid nanoparticles in 8-fold lower concentration than the pristine AgNPs, inhibit QS-regulated virulence factors and reduce by 100 % the *P. aeruginosa* biofilm formation.

**Antibacterial and antibiofilm acylase/aminocellulose/silver NPs**

Aleksandra Ivanova, Kristina Ivanova, Antje Tied, Thomas Heinze, and Tzanko Tzanov*

**Layer-by-Layer Coating of Aminocellulose and Quorum Quenching Acylase on Silver Nanoparticles Synergistically Eradicate Bacteria and Their Biofilms**

**Table of contents**